Published OnlineFirst July 22, 2015; DOI: 10.1158/1078-0432.CCR-15-0393

Cancer Therapy: Clinical

Clinical Cancer Research

Cellular Mechanisms Underlying Complete Hematological Response of Chronic Myeloid Leukemia to BRAF and MEK1/2 Inhibition in a Patient with Concomitant Metastatic Melanoma

Miles C. Andrews[1,2,3,4,5], Natalie Turner[1,2,6], Janis Boyd[7], Andrew W. Roberts[5,6,7], Andrew P. Grigg[5,8], Andreas Behren[2,3,4], and Jonathan Cebon[1,2,3,4]

Abstract

Purpose: Targeted MEK inhibition is an emerging therapy in a number of solid tumors. It holds particular promise in BRAF V600E mutation–positive malignant melanoma, where constitutive activation and cell growth through the MAP kinase (MAPK) pathway is well established. *In vitro* and preclinical research indicates that MAPK pathway activation is important in chronic myeloid leukemia (CML) leukemogenesis; however, the potential of MEK inhibition has not yet been investigated clinically in the setting of such hematologic malignancies.

Experimental Design: We report a case of complete hematologic response of CML to MEK inhibition in a patient with synchronous metastatic melanoma, who received treatment with combination BRAF and MEK1/2 inhibitors. We studied the effects of these agents on proliferation and outgrowth of myeloid precursors, and longitudinal shifts in peripheral blood phenotyping during the course of treatment. A model cell line system was used to examine the effects of dabrafenib and trametinib on MAPK and BCR–ABL1 signaling.

Results: After 35 weeks on treatment with BRAF and MEK inhibitors, complete hematologic response was observed without recourse to BCR–ABL1–targeted therapy. MEK inhibition was principally responsible for impaired proliferation of both mature and primitive myeloid precursors, as well as growth and hemoglobinization of erythroid precursors. Paradoxical activation of the MAPK pathway was seen in response to BRAF inhibitor therapy but this was easily overcome by clinically relevant doses of concurrent MEK inhibitor.

Conclusions: These studies suggest that further evaluation of the optimal MAPK targeting approach is warranted to extend therapeutic options in CML. *Clin Cancer Res; 21(23); 5222–34. ©2015 AACR.*

Introduction

Chronic myeloid leukemia (CML) is almost universally characterized by a reciprocal translocation between the breakpoint cluster region (*BCR*) gene on chromosome 22, and the Abelson murine leukemia viral oncogene homolog 1 (*ABL1*) gene on chromosome 9, resulting in constitutive expression of a BCR–ABL1 fusion protein (1, 2). Imatinib, a small-molecule tyrosine kinase inhibitor that binds to and sterically interferes with the kinase domain of BCR–ABL1, effectively halts its constitutive and oncogenic cell-cycle signaling activity. Kinase inhibition, as typified by imatinib (3), now forms a major part of the therapeutic options in molecularly based subtypes of advanced lung, breast and medullary thyroid cancers, melanoma, gastrointestinal stromal tumors, and hematologic malignancies such as CML.

On the basis of high rates of oncogenic activating *BRAF* mutations, current kinase inhibitor-based therapy in melanoma is centered upon targets within the MAP kinase (MAPK) signaling pathway. Because of the importance of MAPK signaling in virtually all tissues of the body, effects of these inhibitors on nonmalignant cells has become a field of intense research.

The MAPK pathway is also known to be an important mitogenic signaling cascade in leukocytes, and its role in myeloproliferative disease is being increasingly established; however, the precise effects of MAPK inhibitors are highly dependent on the specific clinical context in which these agents are used. MEK inhibition has been demonstrated to rapidly correct aberrant myeloproliferative activity seen in murine models of both chronic and juvenile myelomonocytic leukemia, relating to MAPK hyperactivity induced by an activating *KRAS* mutation (4) or inactivation of the *NF1* tumor-suppressor gene (5). Other studies have revealed that RAS-driven MAPK pathway dependence may be inadvertently intensified by BCR–ABL kinase inhibitors, leading to a synergistic antileukemic effect when used in combination with a MEK inhibitor (6). Similarly, a case of accelerated *RAS*-

[1]Medical Oncology, Austin Health, Austin Hospital, Heidelberg, Victoria, Australia. [2]Ludwig Institute for Cancer Research, Austin Branch, Heidelberg, Victoria, Australia. [3]Olivia Newton-John Cancer Research Institute, Heidelberg, Victoria, Australia. [4]School of Cancer Medicine, La Trobe University, Heidelberg, Victoria, Australia. [5]Faculty of Medicine, Dentistry and Health Sciences, University of Melbourne, Parkville, Victoria, Australia. [6]The Walter and Eliza Hall Institute of Medical Research, Parkville, Victoria, Australia. [7]Clinical Haematology and Bone Marrow Transplantation, Royal Melbourne Hospital, Parkville, Victoria, Australia. [8]Haematology, Austin Health, Austin Hospital, Heidelberg, Victoria, Australia.

Note: Supplementary data for this article are available at Clinical Cancer Research Online (http://clincancerres.aacrjournals.org/).

Corresponding Author: Jonathan Cebon, Olivia-Newton John Cancer Research Institute, Level 5, ONJCWC, 145 Studley Road, Heidelberg, VIC 3084, Australia. Phone: 61-3-9496-5462; Fax: 61-3-9457-6698; E-mail: jonathan.cebon@onjcri.org.au

doi: 10.1158/1078-0432.CCR-15-0393

Published OnlineFirst July 22, 2015; DOI: 10.1158/1078-0432.CCR-15-0393

Translational Relevance

Despite radically altering the treatment and prognosis of chronic myeloid leukemia (CML), BCR-ABL–targeted tyrosine kinase inhibitors are frequently limited by the development of resistance or intolerable toxicity. A number of preclinical studies have demonstrated a potential role for MAP kinase (MAPK) inhibition, principally in drug-resistant CML, but clinical data are lacking. We describe a complete hematologic response to MEK inhibition in a patient with CML who notably did not receive conventional BCR-ABL kinase inhibitor therapy. We demonstrate the sensitivity of myeloid and erythroid progenitor outgrowth to MEK inhibition and place this in the context of what is currently known about BCR-ABL and MAPK pathway signaling. These findings support further clinical evaluation of the therapeutic role for MEK inhibition, not limited to the setting of conventional BCR-ABL kinase inhibitor resistance.

mutant leukemia was reported in a patient with metastatic melanoma receiving treatment with a BRAF inhibitor (7).

We report the case of a patient with BRAF V600E metastatic malignant melanoma who was treated with a combination of the V600-mutation–specific BRAF inhibitor dabrafenib, and the MEK1/2 inhibitor trametinib. Incidentally, he had a synchronous diagnosis of t(9;22) positive CML with an initial circulating leukocyte count of >100 $\times$ 10^9/L. Despite not receiving BCR–ABL–targeted kinase inhibitor therapy, he achieved hematologic complete remission while on dabrafenib and trametinib treatment. Correlative *ex vivo* and *in vitro* analyses confirmed a dominant effect of the MEK inhibitor rather than the BRAF inhibitor on the patient's leukocytes, mediated by a relatively selective reduction in cell number and MAPK signaling within precursor (primitive) cell populations and reduced colony-forming potential. We also demonstrate that in CML cells, in contrast to several solid tumor types, the addition of a MEK inhibitor is able to overcome the paradoxical MAPK activation induced by BRAF inhibition. These findings suggest that further investigation of the role of MAPK pathway inhibition in *de novo* CML in a clinical setting is warranted.

Materials and Methods

Patient details

The patient was enrolled in a phase I/II clinical trial of dabrafenib and trametinib in advanced melanoma (BRF113220, GlaxoSmithKline, ClinicalTrials.gov number NCT01072175; ref. 8), approved by the Institutional Review Board of Austin Health, Australia (Austin Health Human Research Ethics Committee, project number H2011/03955). All patient-derived tissue/blood samples were provided voluntarily under the auspices of the Cancer Biobanking and Research protocol approved by the Institutional Review Board of Austin Health, Australia (H2012/04446), to which the patient had previously consented. Blood samples were collected at multiple time points prior to, during, and after the patient's period of treatment with kinase inhibitors for metastatic melanoma. Baseline leukocyte samples were also obtained from peripheral blood leukapheresis. Clinical follow-up data were as per trial protocol and standard clinical care.

Methods

Hematologic monitoring. Differential cell counts and blood films were obtained from diagnostic blood samples collected and analyzed through the local pathology service provider (Austin Pathology). Cytogenetic analyses were performed by the Victorian Cytogenetics Service, and *BCR–ABL1* counts performed at the Royal Melbourne Hospital (Parkville, VIC, Australia).

Flow cytometry. To estimate the effects of *in vivo* kinase inhibitor treatment on MAPK signaling in leukocyte subsets, peripheral blood mononuclear cells (PBMC) isolated from blood samples taken at baseline, week 8 and week 20, were subjected to multicolor flow cytometry. Two stains were applied: a "monocytic" stain, comprising CD45 (Cy5; BD Pharmingen; cat. no. 555484), CD34 (PE-Cy7; Beckman Coulter PN A51077 clone 581), HLA-DR (FITC; BD Pharmingen; cat. no. 555811), CD14 (APC; Beckman Coulter IM2580 clone RMO52), pERK (PE; Cell Signaling Technology; #5682S) or equivalent isotype controls, and live/dead stain (Pacific Blue, LIVE/DEAD fixable violet dead cell stain, Invitrogen L34955); and a "myeloid" stain, comprising CD45, CD34, HLA-DR, CD11b (APC; BD Pharmingen; cat. no. 550019), CD16 (APC-Alexa Fluor750; Beckman Coulter PN A66330 clone 3G8), pERK, or isotype controls, and live/dead stain. All cells were gated on forward and side-scatter characteristics, live cells, and $CD45^+$ cells. Subpopulations of interest included blast ($CD34^+/HLA^-DR^+$), immature/promonocyte ($CD34^-/HLA^-DR^-/CD14^-$), mature monocyte ($CD34^-/HLA^-DR^-/CD14^+$), myelocytes ($CD34^-/HLA^-DR^-/CD11b^+/CD16^-$) and metamyelocytes/mature neutrophils ($CD34^-/HLA^-DR^-/CD11b^+/CD16^+$). MAPK pathway activation status was measured by both the proportion of cells staining positive for phosphorylated ERK1/2 (pERK) relative to isotype control, and comparison of relative pERK staining intensities between time points in monocytic and myeloid lineage cells.

Cell line culture. Three BCR–ABL harboring cell lines were used for *in vitro* studies. K562 (BCR-ABL b3-a2 fusion) was obtained from institutional stocks, MEG-01 (BCR-ABL b2-a2) was a gift from Dr. Ashley Ng (Walter and Eliza Hall Institute, Parkville, VIC, Australia), and KU-812 (BCR-ABL b3-a2 fusion) was obtained from Cell Bank Australia (Westmead, NSW, Australia); identity was confirmed by short-tandem repeat (STR) profiling. All cell lines were maintained in semiadherent culture in RPMI-1640 media (Gibco, Life Technologies, Mulgrave VIC, Australia) supplemented with 10% fetal bovine serum (Sigma), 1% glutamine (glutaMAX) and 1% penicillin/streptomycin (both from Gibco, Life Technologies) and incubated in 5% atmospheric CO_2 at 37°C.

In vitro proliferation assays. *In vitro* analysis of kinase inhibitor effects on proliferation was performed using the K562 leukoerythroblastic cell line. Cells were plated out at seeding densities of 4,000 cells per well in 96-well plates and treated with dabrafenib at doses of 0, 0.01, 0.1, 1, or 5 μmol/L, trametinib at doses of 0, 0.1, 1, 10, or 100 nmol/L, or their respective combinations, for a period of 72 hours. The doses used were chosen to cover the typically achieved human plasma concentrations *in vivo*. Proliferation was determined colorimetrically by addition of MTS reagent (1 in 6 dilution of CellTiter 96 AQueous One Solution Cell Proliferation Assay; Promega), incubation for 1.5 hours, measurement of the absorbance at 490 nm, and

Published OnlineFirst July 22, 2015; DOI: 10.1158/1078-0432.CCR-15-0393

comparison to the absorbance in untreated cells following background correction.

Colony-forming assays. DMSO-cryopreserved aliquots of leukapheresis samples collected prior to commencement of any tyrosinase kinase inhibitor (TKI) were thawed, resuspended in IMDM/10%FCS, and then cultured, as previously described in detail (9). Cultures were set up at 5×10^4 cells/mL in 0.3% Bacto Agar (Becton Dickinson; #214010), 25% fetal bovine serum (Gibco; Life Technologies) and IMDM (Invitrogen; containing glutamine, 2-mercaptoethanol, asparagines, and DEAE Dextran) in a fully humidifed 5%CO_2/air atmosphere before scoring. Day 7 colony-forming cells (CFC; mature myeloid progenitors) were scored if >30 cells were present, and 14 day BFU-E and GM-CFC (immature erythroid and myeloid progenitors, respectively) were scored if >50 cells were present. Day 7 cultures were stimulated with G-CSF (2,000 U/mL (Neupogen, Amgen), and day 14 cultures with GM-CSF (100 ng/mL; R&D Systems Inc.), IL3 (100 ng/mL; R&D Systems Inc.), SCF (100 ng/mL; R&D Systems Inc.), and erythropoietin (200 ng equivalent to 4 U/mL; Aranesp, Amgen). Cultures were in triplicate for initial titrations and duplicate for mixture experiments. EC_{50}s were calculated from log-transformed normalized data using GraphPad Prism software (GraphPad Software Inc.).

Western blotting. For *in vitro* phosphoprotein studies, K562, MEG-01, and KU-812 cells were resuspended in serum-free media, allowed to equilibrate for 30 minutes, and subsequently plated into 6-well plates (1.5×10^6 cells/well) containing imatinib mesylate, dabrafenib, trametinib, or DMSO only (vehicle control, 0.1%–0.2%) to the final doses as indicated in results. Cells were incubated for 2 hours prior to harvest and lysis in RIPA buffer (Pierce) containing the manufacturer's recommended concentrations of PhosSTOP phosphatase inhibitor and cOmplete ULTRA EDTA-free protease inhibitor (Roche Diagnostics GmbH). Protein concentrations were estimated using the BCA method (Thermo Scientific Pierce BCA Protein Assay Kit; cat. no. 23225) and samples adjusted to uniform final concentrations, prior to the addition of NuPAGE LDS Sample Buffer (×4) and NuPAGE sample reducing agent (×10; both from Novex; Life Technologies; cat. nos. NP008 and NP009). Samples were electrophoresed on NuPAGE Novex Bis–Tris 4% to 12% precast gels with SeeBlue Plus2 prestained protein standard (Novex; Life Technologies) prior to transfer to nitrocellulose membrane by dry (iBlot Dry Blotting System, Invitrogen), or semi-wet (Invitrogen XCell II Blot Module; cat. no. EI9051) methods as necessary for optimal transfer. Erk phosphorylation was determined using mouse anti-human p44/42 MAPK (Erk1/2; 3A7) at 1:2,000, rabbit anti-human phospho-p44/42 MAPK (Erk1/2; Thr202/Tyr204; 197G2) at 1:2,000, and rabbit anti-human α/β-tubulin at 1:2,000 (Cell Signaling Technology; cat. nos. 9107, 4377, 2148) followed by IRDye 680RD goat anti-mouse IgG and IRDye 800CW goat anti-rabbit IgG secondaries at 1:40,000 and 1:20,000, respectively (LI-COR, Prod. Nos. 926-68070 and 926-32211). BCR–ABL1 activity was measured using the PathScan Bcr/Abl Activity Assay cocktail (1:500; Cell Signaling Technology; cat. no. 5300) consisting of rabbit antibodies raised against phospho-c-Abl (Tyr245), phospho-Stat5 (Tyr694), phospho-CrkL (Tyr207), and Rab11 (loading control), followed by anti-rabbit antibody as above. Wet-transfer combination treatment blots also contained mouse anti-human β-actin (1:3,000) primary followed by goat anti-mouse secondary as above as an additional loading control. After staining, membranes were dried and scanned on the LI-COR ODYSSEY Infrared Imaging System and densitometry performed in the ODYSSEY software. Densitometry results were normalized to Rab11 (ABL activity assay); ERK phosphorylation was expressed as the ratio of phosphorylated to total ERK1/2 and normalized to nontreated (DMSO) control.

For analysis of BIM isoform protein expression following kinase inhibitor treatment, K562, MEG-01, and KU-812 cells were incubated in full-serum media for 24 hours in the presence of imatinib, dabrafenib, and/or trametinib at doses indicated in the results, prior to harvest and processing as described above. Following transfer to nitrocellulose membranes usin the iBlot system, membranes were probed with mouse anti-β-actin (as above) and a rabbit monoclonal anti-BIM antibody [Y36] at 1:1,000 (ab32158; Abcam), followed by secondary staining and visualization as above. For brevity, where blots have been displayed in figures, only relevant bands of confirmed correct size according to markers are shown.

Results

Case report

A 26-year-old man with a history of moderately severe psoriasis managed with topical steroids and prior PUVA therapy, was diagnosed with stage IIIB malignant melanoma (10) of unknown primary, involving the left inguinal lymph nodes. He underwent a left groin lymph node dissection, followed by resections of left upper thigh subcutaneous and left iliac lymph node recurrences within 6 months. He received local postoperative radiotherapy after the second recurrence. A further 10 months later he underwent resection of a solitary right lower lobe pulmonary metastasis detected on routine surveillance imaging. Surveillance FDG-PET scan performed 4 months later confirmed relapsed disease with multiple metastases involving the left adrenal, bone, lymph nodes, subcutaneous sites, and liver. At that time the patient was asymptomatic, with an Eastern Cooperative Oncology Group (ECOG) performance status (11) of 0 (unrestricted function).

Genetic testing performed on the previously resected lung metastasis identified a V600E mutation in the *BRAF* gene. The patient was considered for enrollment in a phase I/II clinical trial of combination BRAF and MEK inhibitors in advanced melanoma (BRF113220, GlaxoSmithKline, clinical trial identifier NCT01072175). Screening investigations performed as per trial protocol demonstrated a markedly elevated white cell count (WCC) of 109×10^9/L, with a left-shifted white cell differential. No eosinophilia or basophilia were reported per the automated analyzer differential. Hemoglobin was 106 g/L, and the platelet count was 145×10^9/L. The blood film showed a leukoerythroblastic picture with marked leukocytosis and occasional tear-drop cells, with no other specific features. Other than an elevated LDH of 579 (normal range, 98–192 IU/L), biochemistry results, including electrolytes, urea, and creatinine and liver enzymes, were within normal limits. The patient had no known medical history of blood dyscrasias and was unaware of any previous abnormal blood investigations. Of note, a full blood count (FBC) sample taken at the time of the lung metastectomy, which had been performed at a different institution, was subsequently located. This showed normal hemoglobin and platelet counts, mild leukocytosis with total

Published OnlineFirst July 22, 2015; DOI: 10.1158/1078-0432.CCR-15-0393

WCC 25 $\times$ 10^9/L, with a left-shifted differential, and no eosinophilia or basophilia.

The marked leukocytosis was initially considered to be a leukemoid reaction caused by paraneoplastic release of G-CSF secondary to metastatic melanoma (12), and the leukoerythroblastic film attributed to marrow involvement with melanoma. Peripheral blood was sent for molecular analysis, although results for this were anticipated to take at least 1 week. Given the rapidity with which the patient had relapsed and the high burden of metastatic disease, commencement on therapy was considered a higher clinical priority. The patient was enrolled in the BRF113220 clinical trial and randomized to receive both the BRAF inhibitor dabrafenib (GSK2118436, 150 mg twice daily), and the MEK-inhibitor trametinib (GSK1120212, 2 mg daily). Treatment commenced immediately following a cytoreductive leukapheresis.

One week after starting on trial therapy, molecular analysis of peripheral blood was completed and demonstrated the presence of *BCR–ABL1* t(9;22) fusion gene, with both a major b2-a2 (p210) transcript, and a minor e1-a2 (p190) transcript detectable. A subsequent manual review of the baseline blood film and repeat differential noted mild eosinophilia and basophilia. A bone marrow biopsy confirmed a diagnosis of CML in chronic phase, and did not show evidence of infiltration by melanoma. Cytogenetic analysis demonstrated t(9;22)(q34;q11.2) without additional abnormalities or evidence of deletion of the derivative chromosome 9.

Despite this concomitant diagnosis, as the patient's overall prognosis was deemed to be more significantly affected by metastatic melanoma than CML he was permitted to remain on trial protocol therapy, providing that he did not commence imatinib for treatment of the CML concurrently, given the lack of safety data for the combination of dabrafenib/trametinib with other kinase inhibitors. As CML was in chronic phase and was to be monitored closely with weekly FBC and regular Hematology review, he continued on trial.

The patient initially tolerated BRAF- and MEK-inhibitor therapy without any adverse effects and performance status remained excellent. Despite lack of specific therapy for CML, total WCC decreased within 4 weeks of commencing on trial treatment, and continued to decline over the subsequent 6 months (Fig. 1). High resolution melt curve analysis of the patient's leukocytes confirmed the absence of a BRAF V600 mutation.

Restaging for melanoma after 8 weeks on trial demonstrated a partial response by RECIST 1.1 criteria (13), and at week 16 he had a near-complete response on CT imaging together with a complete metabolic response on FDG-PET imaging. At week 24, the patient developed a solitary site of melanoma progression in a left adrenal metastasis, but remained on trial due to continuing clinical benefit with ongoing good control of melanoma at all other sites.

During enrollment on trial, the patient required two treatment breaks. The first occurred at week 24 due to development of asymptomatic reduction in left ventricular ejection fraction. Both inhibitors were withheld for 4 weeks as per study protocol. Left ventricular dysfunction resolved without specific intervention and dabrafenib and trametinib were restarted with a protocol-mandated 25% dose reduction of trametinib.

The second treatment break occurred at week 38, at the time that the patient underwent elective laparoscopic left adrenalectomy for treatment of the solitary progressing metastasis. After a period of 48 hours following surgery, both inhibitors were recommenced at the same doses.

Weekly FBC monitoring throughout treatment confirmed a normalized WCC of 8.4 $\times$ 10^9/L after 35 weeks on trial, with associated resolution of the left-shifted myeloid series, eosinophilia and basophilia (Supplementary Table S1), consistent with a complete hematologic response. Nevertheless, repeat PCR in peripheral blood for the *BCR–ABL1* fusion gene showed persistently detectable levels (Supplementary Table S2). Following left adrenalectomy, total WCC increased, peaking at week 41 (Fig. 1 and Supplementary Table S2) with associated recurrence of a left-shifted differential. At the same time, the patient experienced a significant flare of psoriasis that required temporary intensification of topical agents (calcipotriol/betamethasone).

Hematologic monitoring

Temporal trends in the patient's WCC, differential and blood/bone marrow *BCR–ABL* levels are shown in Fig. 1 and Supplementary Tables S1 and S2. Rather than a proportional cytoreduction in WCC, there was a greater reduction in myelocyte, promyelocyte, eosinophil, and blast cell numbers than lymphocyte subtypes. Following the 4-week break from dabrafenib/trametinib therapy (weeks 24–28), myeloid cells at varying stages of maturation increased in number. Total WCC again peaked approximately 3 weeks following adrenalectomy, consisting largely of myelocytes, metamyelocytes, and band neutrophils, potentially suggesting a left-shift precipitated by perioperative stress.

The patient ceased kinase inhibitors late in week 48 due to clear progression of his melanoma. At that time, CML remained well controlled with a circulating leukocyte count of 14.0 $\times$ 10^9/L. The patient subsequently received several lines of cytotoxic chemotherapy with resultant multilineage cytopenias, confounding ongoing interpretation of CML behavior.

Ex vivo analysis of leukocyte subsets and MAPK signaling

Representative FACS plots and gates for the monocytic and granulocytic stains are shown in Supplementary Fig. S1. Proportions of cells within each defined subpopulation are shown in Supplementary Table S3; due to the relative depletion of mature myeloid cells during standard Ficoll-based PBMC isolation, the constituent leukocyte subpopulations observed by flow cytometry differ markedly from those seen in contemporaneous peripheral blood films and are likely unreliable for more mature granulocytic populations. $CD34^+/HLA^-DR^+$ blast numbers declined by over 6-fold from baseline to week 20 ($P < 0.0001$, one-way ANOVA; Fig. 2A). The proportion of blasts with measurable levels of pERK declined at week 8 and remained low at week 20 ($P = 0.0014$ across all time points, one-way ANOVA; Fig. 2B; Supplementary Table S3). pERK staining intensity remained stable as measured by the mean fluorescence intensity (MFI) of pERK-PE (Supplementary Table S3). Mature monocytes were almost entirely (>99.0%) positive for pERK at all time points (Supplementary Table S3); however, the mean intensity of pERK staining increased significantly from baseline to week 20 (3,949 vs. 4,735). This may be due to the uneven separation of cells into pERK-high or -low subpopulations (Fig. 2C).

Cell staining to define myeloid/granulocytic maturation stages demonstrated similar results for the $CD34^+/HLA^-DR^+$ blast population as were seen in the monocytic stain series (Supplementary Table S3). Myelocyte ($CD34^-/HLA^-DR^-$/

Published OnlineFirst July 22, 2015; DOI: 10.1158/1078-0432.CCR-15-0393

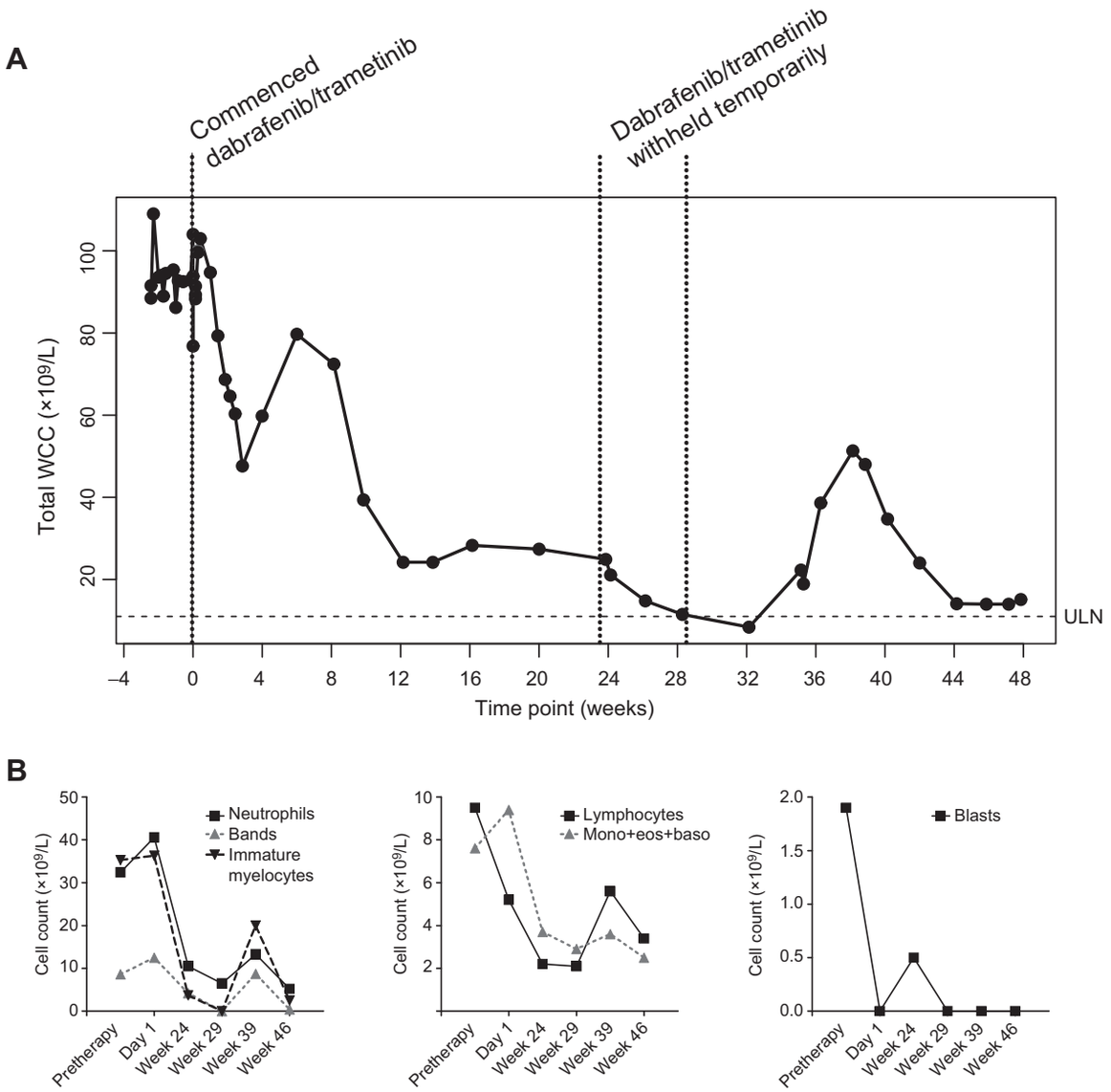

Figure 1.
Evolution of peripheral blood total and differential WCCs during treatment for metastatic melanoma. A, total WCC, and B, differential cell counts from peripheral blood samples taken throughout the patient's treatment period; mono+eos+baso indicates the combined count of monocytes, eosinophils, and basophils. Critical clinical events and the upper limit of normal (ULN) of total WCC are indicated in A.

$CD11b^+/CD16^-$) pERK positivity reduced progressively from baseline to week 20 ($P = 0.0001$, one-way ANOVA; Fig. 2D; Supplementary Table S3) together with a greater than 50% reduction of mean pERK signal intensity (Fig. 2E). Metamyelocyte ($CD11b^+/CD16^+$) pERK-positive proportions fluctuated moderately, with no sustained trend in pERK staining intensity over the observed time points (Fig. 2F and Supplementary Table S3).

Effects of BRAF and MEK inhibitor therapy on colony formation

Next, the effect of each kinase inhibitor on hematopoietic progenitor cells from the patient was analyzed. Tested dose ranges of either drug were chosen to encompass typically achieved maximal plasma concentrations *in vivo*, namely 1 to 2 μmol/L for dabrafenib and 10 to 30 nmol/L for trametinib. Both drugs inhibited the formation of colony formation from leukapheresis mononuclear cells in a dose-dependent fashion (Fig. 3). Trametinib was significantly more potent than dabrafenib for each colony type analyzed. Both mature (day 7 CFC) and more primitive myeloid progenitors (day 14 GM-CFC) were inhibited by concentrations of trametinib achievable *in vivo*. Primitive erythroid progenitors (BFU-E) displayed similar sensitivity to trametinib; hemoglobinization and size of individual colonies were also significantly negatively affected in a dose-dependent fashion. Next, the effects of coincubation of trametinib with dabrafenib at two fixed concentrations achievable *in vivo* were tested. Divergent behavior was observed according to the type of

Published OnlineFirst July 22, 2015; DOI: 10.1158/1078-0432.CCR-15-0393

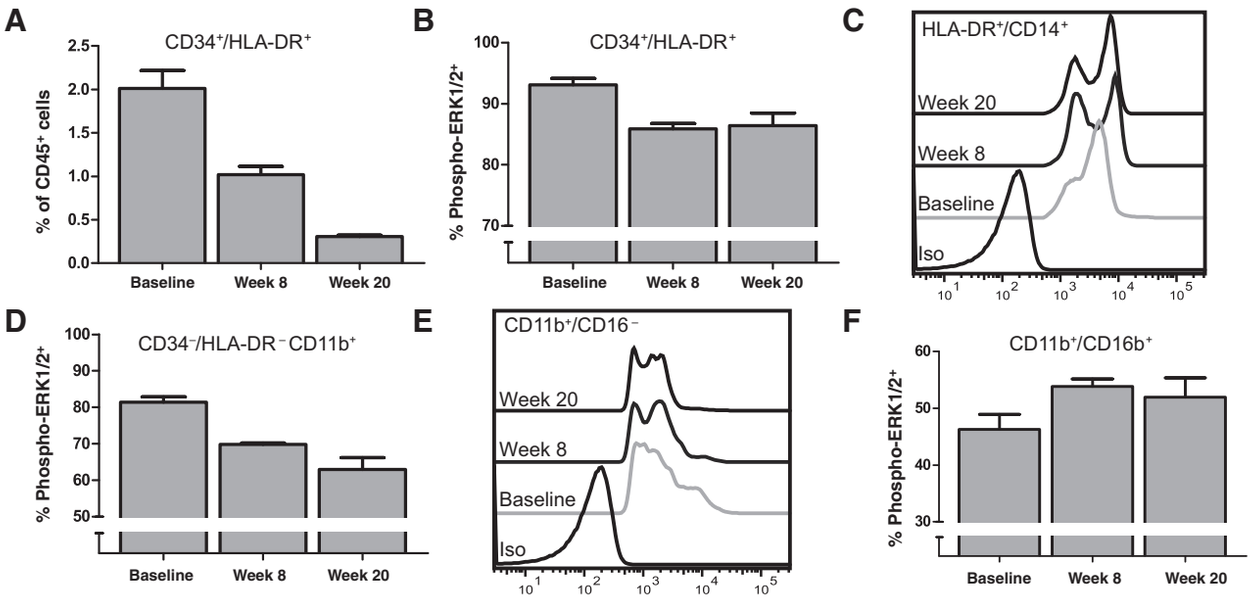

Figure 2.

Flow cytometric analysis of leukocytes collected from the patient at baseline, prior to commencement of kinase inhibitor therapy (baseline), and again at week 8 and week 20 of therapy. A, $CD34^+/HLA^-DR^+$ blast-like cells decreased in number (expressed as a percentage of $CD45^+$ cells) over time, coincident with a reduction in the percentage of cells bearing detectable amounts of phospho-ERK1/2 (B). Mature monocytic forms ($CD14^+$) also appeared to split into two pERK-positive subpopulations with a bias toward higher-intensity staining (C). Myelocytes ($CD11b^+/CD16^-$) showed a reduction in pERK positivity (D) due largely to a loss of right-skewing in the distribution of PE stain intensity over time (E). Metamyelocytes ($CD11b^+/CD16^+$) showed no consistent trend in pERK staining positivity over time.

progenitor cell being assayed. Dabrafenib had no significant effect on BFU-E and GM-CFC sensitivity to trametinib (Fig. 3B). However, for more mature day 7 myeloid CFC, dabrafenib 1.25 μmol/L demonstrated an additive effect with trametinib on the inhibition of day 7 CFC progenitor cell growth, with the calculated half-maximal effective concentration (EC_{50}) for trametinib reducing from 17 nmol/L (95% CI, 13–23) to 4 nmol/L (95% CI, 3–6). In contrast, in the presence of 0.31 μmol/L dabrafenib, the calculated half-maximal effective concentration (EC_{50}) of trametinib was higher, 32 nmol/L (95% CI, 25–42) than for trametinib alone, suggesting partial antagonism (Fig. 3B).

Effect of BRAF and MEK inhibition on K562 cell line proliferation

Because of limited available patient-derived sample, the effect of the BRAF and MEK1/2 inhibitors was then evaluated further in a BCR-ABL–dependent leukemic cell line, K562. Proliferation curves at constant trametinib dose (Fig. 4A) indicate the relative lack of effect of dabrafenib on proliferation unless cells are cotreated with clinically relevant doses of trametinib (≥1 nmol/L; black lines). Very high doses of trametinib (100 nmol/L) produced >50% inhibition of cellular proliferation with minimal additional contribution from dabrafenib at any dose.

Similarly, the effect of up-titrating trametinib in combination with each given dose of dabrafenib (Fig. 4B) clearly demonstrates the dominance of trametinib in driving a dose-dependent inhibition of proliferation.

Notably, at low dabrafenib doses (<1 μmol/L), the inhibitory effect of trametinib on proliferation was reduced relative to dabrafenib-untreated cells (Fig. 4A), while at higher dabrafenib doses of 1 and 5 μmol/L there was additive antiproliferative effect. This biphasic effect is consistent with the *in vitro* analyses of the patient's mature myeloid progenitor cells (i.e., day 7 CFC).

Overall, there was a dominant antiproliferative effect of kinase inhibitor therapy mostly attributable to the effect of trametinib at clinically relevant doses. This is consistent with a MEK-mediated effect in this cell line that lacks an activating BRAF V600 mutation.

Effects of BRAF and MEK inhibition on BCR–ABL1 and MAPK pathway activity

As expected, imatinib treatment of K562 cells markedly reduced phosphorylation of BCR–ABL1 with consequent downstream reduction of STAT5 phosphorylation and ERK1/2 phosphorylation, confirming that the MAPK pathway responds to upstream modulation of BCR–ABL1 activity (Fig. 5A). Trametinib monotherapy for 2 hours in K562 cells inhibited ERK1/2 phosphorylation relative to basal (untreated) conditions in a dose-dependent manner. Consistent with potential paradoxical activation of MEK/ERK signaling in RAS-activated cells that lack activating BRAF V600 mutations, dabrafenib monotherapy markedly increased ERK1/2 phosphorylation with a maximal response between 0.5 and 1 μmol/L (Fig. 5A and B). In combination with dabrafenib, trametinib doses attenuated (1 nmol/L) or abrogated (10–100 nmol/L) this paradoxical activation, and reduced ERK phosphorylation to below basal levels (Fig. 5C and D). These findings were further confirmed in studies of the MEG-01 and KU-812 cell lines, both of which displayed even greater sensitivity to imatinib with an identical pattern of paradoxical ERK activation in response to dabrafenib, which could be overcome by trametinib cotreatment (Fig. 5E and F).

Published OnlineFirst July 22, 2015; DOI: 10.1158/1078-0432.CCR-15-0393

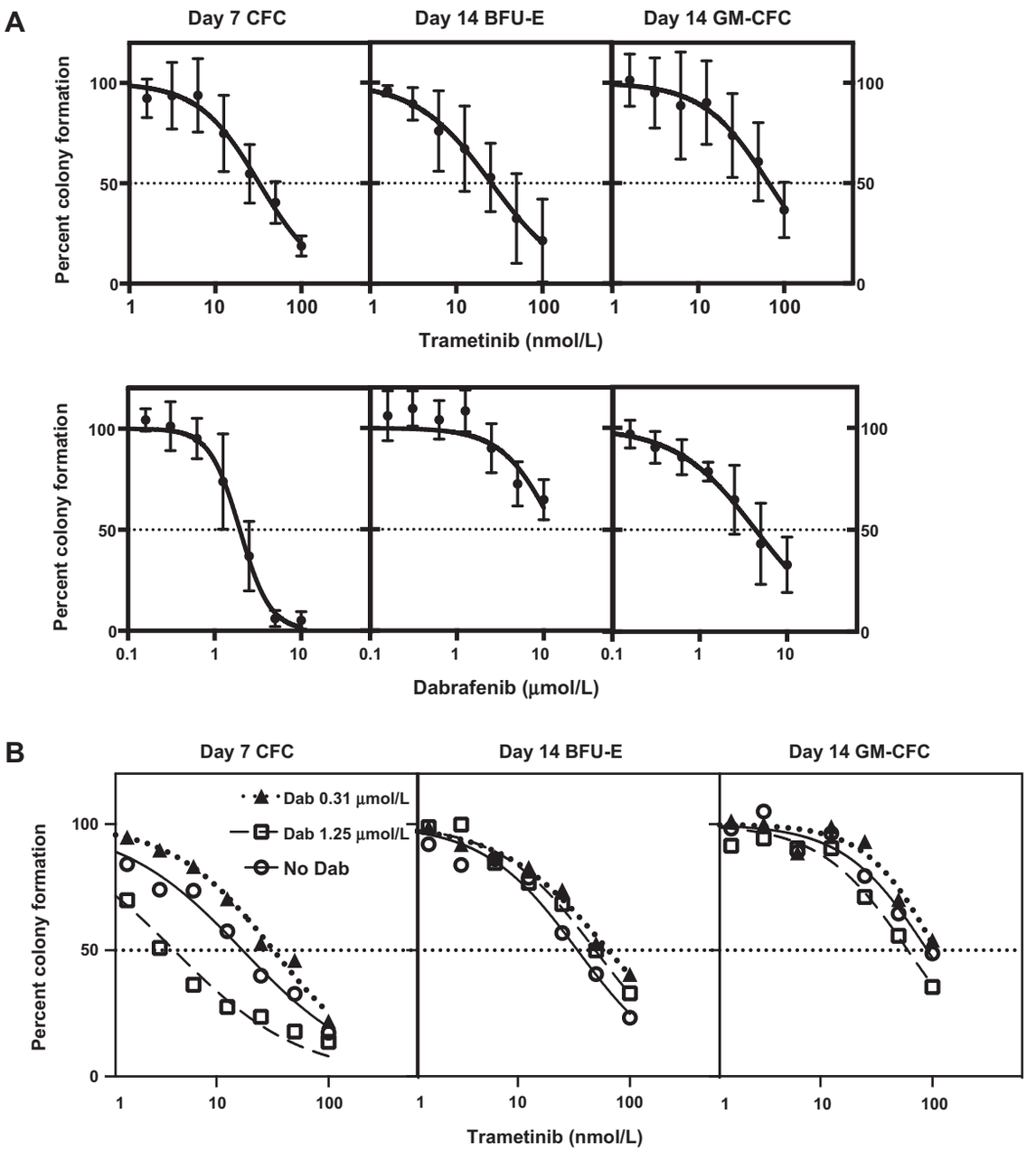

Figure 3.
Sensitivity of myeloid and erythroid colony formation to inhibition with trametinib or dabrafenib or a combination. A, fitted curves and mean ± SEM ($n = 4$ or 5 independent experiments) of normalized log-transformed colony data are shown according to progenitor type for each drug alone. B, effect of combining dabrafenib at two fixed concentrations (0.31 and 1.25 μmol/L) with trametinib at various concentrations is represented by fitted curves. Data are mean of two independent experiments. The half-maximal effective concentration (EC_{50}) for the trametinib titrations were calculated for each fixed dabrafenib concentration and the vehicle control. The only significant differences from vehicle control were observed for day 7 CFC.

To assess for potential direct off-target effects of dabrafenib and/or trametinib on BCR–ABL1 activity, we analyzed phosphorylation of BCR–ABL1, as well as the BCR–ABL1 interacting adaptor protein CRKL and the direct downstream target STAT5 in the same cells used to study ERK phosphorylation. No statistically significant effect on activation of BCR–ABL1 was observed in response to dabrafenib or trametinib treatment, either alone (Fig. 5A and B) or in combination (Fig. 5C and D). Dabrafenib induced a dose-dependent attenuation of STAT5 phosphorylation that was statistically significant for 5 μmol/L dabrafenib ($P < 0.05$ vs. control) although was no longer significant with the addition of trametinib (Supplementary Fig. S2). Neither kinase inhibitor had significant effect on CRKL phosphorylation. Analogous studies in MEG-01 and KU-812 cells using the principal clinically relevant

Published OnlineFirst July 22, 2015; DOI: 10.1158/1078-0432.CCR-15-0393

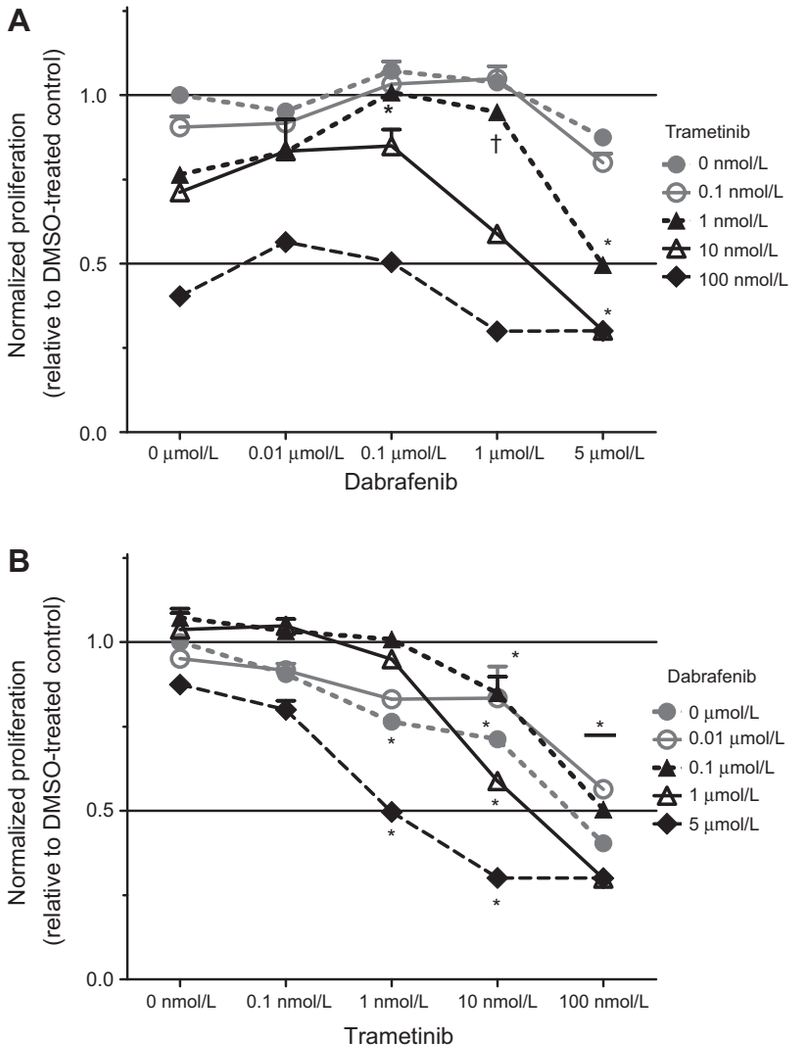

Figure 4.
Effects of dabrafenib and trametinib on proliferation of K562 cells grouped either by (A) constant trametinib dose or (B) constant dabrafenib dose to emphasize the relative contributions of each drug to effects on cellular proliferation. Data are shown as mean ± SEM for three independent replicates normalized to control (DMSO-only treated) cells. Proliferation was significantly influenced by both trametinib dose (67.4% of variance) and dabrafenib dose (19.9% of variance) with evidence of a positive interaction (10.2% of variance) by two-way RM-ANOVA with Bonferroni correction for multiple comparisons; †, $P < 0.01$; *, $P < 0.0001$ within treatment-curves relative to no dabrafenib (A) or no trametinib (B).

doses demonstrated no significant off-target effects of dabrafenib or trametinib on downstream targets of BCR-ABL.

Effects of kinase inhibitors on proapoptotic molecule BIM expression

In all three cell lines tested (K562, MEG-01, and KU-812), BIM-EL was markedly more abundantly expressed than the shorter isoforms (Supplementary Fig. S3). Following 24 hours of exposure to imatinib, increased expression of BIM-EL became evident in K562 (marginally), of all three isoforms in MEG-01, with minimal change in expression of any BIM isoform seen in KU-812 cells (Supplementary Fig. S3). No significant effects on BIM expression were seen with dabrafenib and/or trametinib in K562 or MEG-01 cells; however, dabrafenib in combination with the higher dose of trametinib (10 nmol/L) increased BIM isoform expression in KU-812 cells only.

Discussion

Imatinib is an extremely effective therapy in chronic phase of CML, with over 65% of patients achieving complete cytogenetic response (CCR) after 12 months of therapy and 5-year overall survival rates of approximately 90% (14, 15). Data from the International Randomized Study of Interferon versus STI571 (IRIS) trial comparing IFNα and imatinib (STI571), demonstrated impressive event-free, disease-specific, and overall survival advantages for patients receiving first-line imatinib (16), together with both deep and durable molecular responses, including major metabolic responses (MMR) in 85% to 90% at 5 to 6 years (17). Subsequent generations of inhibitors, such as dasatinib and nilotinib, and more recently ponatinib, are also in clinical use (18). These agents are, however, susceptible to such setbacks as inadequate target specificity, unfavorable side-effect profiles, reduced efficacy due to intra- and intertumoral molecular and genetic heterogeneity, and development of resistance through a variety of mechanisms.

In the present case, a complete hematologic response was seen after a 28-week period of treatment with BRAF and MEK1/2 kinase inhibitors. Concurrently, metastatic melanoma was well-controlled, with near-complete radiologic response by week 16. In addition, the patient ceased kinase inhibitors late in week 48 due to clear progression of his melanoma, despite well-controlled leukocyte counts at that time. Although a humorally mediated

Published OnlineFirst July 22, 2015; DOI: 10.1158/1078-0432.CCR-15-0393

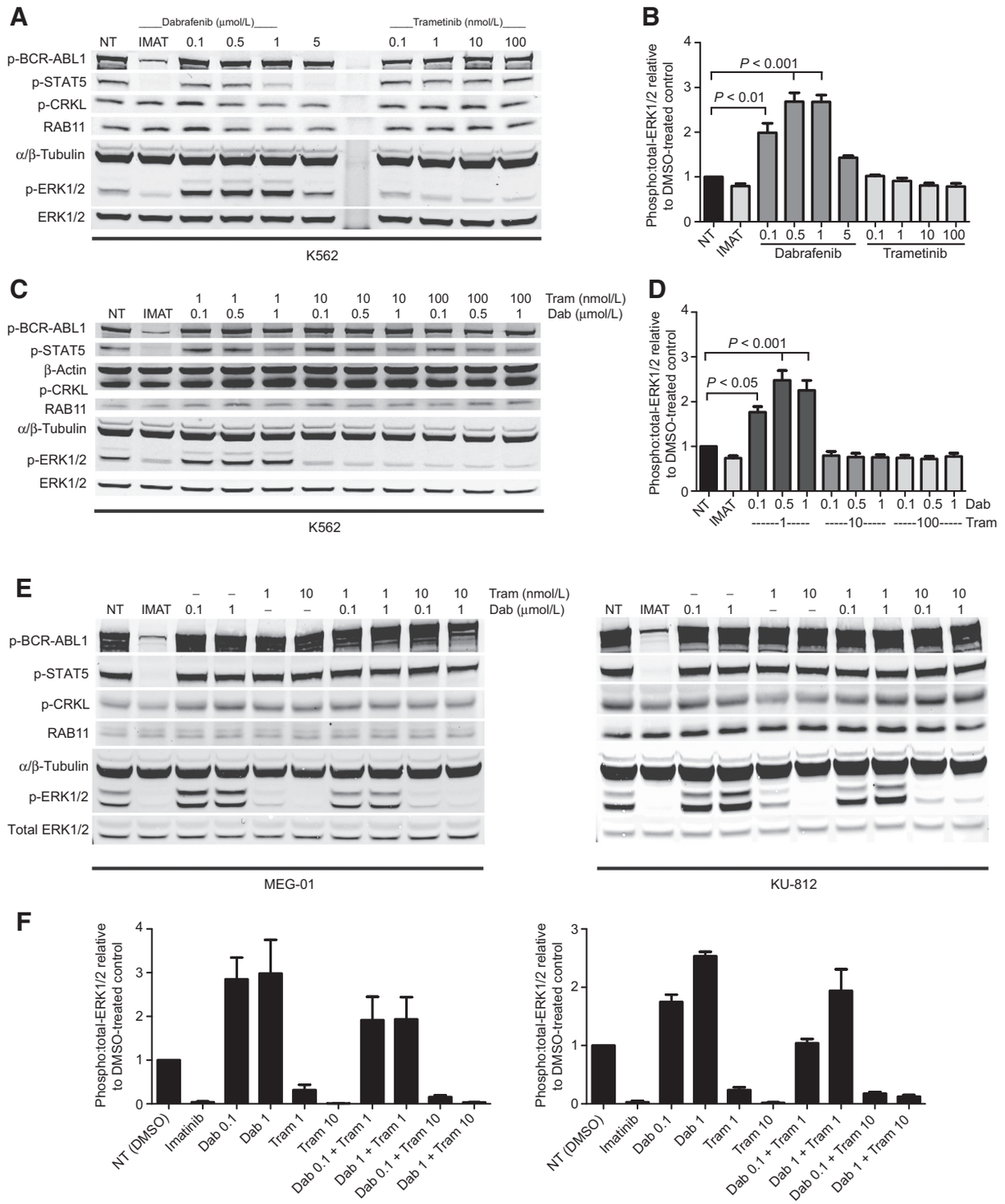

Figure 5.

BCR-ABL activity and ERK phosphorylation were assessed by Western blot analysis following treatment of K562, MEG-01, and KU-812 cells for 2 hours with dabrafenib (Dab) and trametinib (Tram) at the doses indicated. Imatinib (IMAT) was used as a positive control and DMSO-only as a nontreated control (NT); relevant bands from representative blots are shown. A, monotherapy treatments showing dose-dependent reduction of STAT5 phosphorylation by dabrafenib treatment and paradoxical activation of ERK phosphorylation. B, densitometry of phosphorylated:total ERK1/2 shown relative to control ($P < 0.0001$ overall, one-way ANOVA; Tukey multiple comparison method P values vs. control indicated). C, representative blot of combination treatments showing persistent paradoxical activation of ERK phosphorylation only at the lowest concurrent dose of trametinib, confirmed by D) densitometry. E, equivalent BCR-ABL activity and ERK phosphorylation blots using an abbreviated panel of doses in the BCR-ABL harboring cell lines MEG-01 and KU-812, demonstrating minimal effect of dabrafenib or trametinib on BCR–ABL activity, but clear dabrafenib-mediated paradoxical ERK phosphorylation that was ablated by trametinib cotreatment, confirmed by densitometry (F).

effect secondary to the melanoma may have altered the patient's CML disease course, the kinetics of the CML response were delayed and discordant from the melanoma disease course, suggesting a direct antileukemic effect of the BRAF inhibitor, the MEK inhibitor, or both. In particular, the gradual decline in circulating leukocytes and restoration of a normal mature differential count suggests an effect on a primitive or precursor cell population. In support of this, *in vitro* analysis of the patient's leukocytes revealed dose-dependent inhibition of colony formation across multiple precursor cell populations of varying maturity, with a dominant and potent effect of trametinib relative to dabrafenib.

Evaluation of phospho-ERK1/2 levels in patient-derived leukocytes as a surrogate for MAPK pathway activity revealed only modest differences over time in most subpopulations tested, with the exception of myelocytes and mature monocytes. Flow cytometric analysis of patient-derived leukocyte samples is subject to several potential confounding effects on subset enumeration and quantification of residual phosphoprotein levels introduced by sample collection, handling, purification, and freeze-thaw, which largely depleted the dominant circulating cell type (neutrophils) in this patient. Nonetheless, these data suggest that differences in relative sensitivity to MAPK inhibition exist between leukocyte subclasses and maturation stages. Although mature subpopulations were relatively depleted in this analysis, the slow kinetics of response and breadth of cell types affected is most consistent with a more primitive target cell population being ultimately responsible for the observed hematologic response in this patient.

The majority of the antiproliferative effect observed in treatment of the K562 CML cell line was secondary to MEK inhibition, consistent with other studies using MEK inhibitors in this cell line (6, 19–22). Although MEK inhibition appears to have a biphasic dose-response effect on erythroid differentiation in K562 cells (23), it demonstrated a dose-dependent inhibitory effect on erythroid precursors in our patient-derived cells, suggesting a difference in underlying MAPK and erythropoietin receptor (EPO-R) signaling in these differing contexts. In addition, regardless of MEK inhibitor dose, intermediate doses of dabrafenib tended to antagonize the antiproliferative effect of trametinib on K562 cells, resulting in a net proliferation either close to, or higher than control. Western blot analysis demonstrated the paradoxical activation of ERK phosphorylation in K562 cells treated with dabrafenib alone; this effect was dose-dependently reversed by trametinib cotreatment.

Several other studies have demonstrated that pharmacologic inhibition of MAPK signaling can increase cell death and decrease cell proliferation in CML cells *in vitro* (6, 19–22, 24). In a competing fates model of BCR–ABL1 inhibition by inhibitors, such as imatinib and dasatinib, cells typically commit to apoptosis more rapidly than they can restore responses to growth factor–induced survival signals (25). Accordingly, addition of the MEK inhibitor PD184352 to imatinib increased apoptosis in *BCR–ABL1*–positive human myeloid leukemia cells (22) and in another study, enhanced mitochondrial damage and caspase activation following dasatinib treatment, including in cells overexpressing *BCR–ABL1* and in some forms of *BCR–ABL1* point mutations (20).

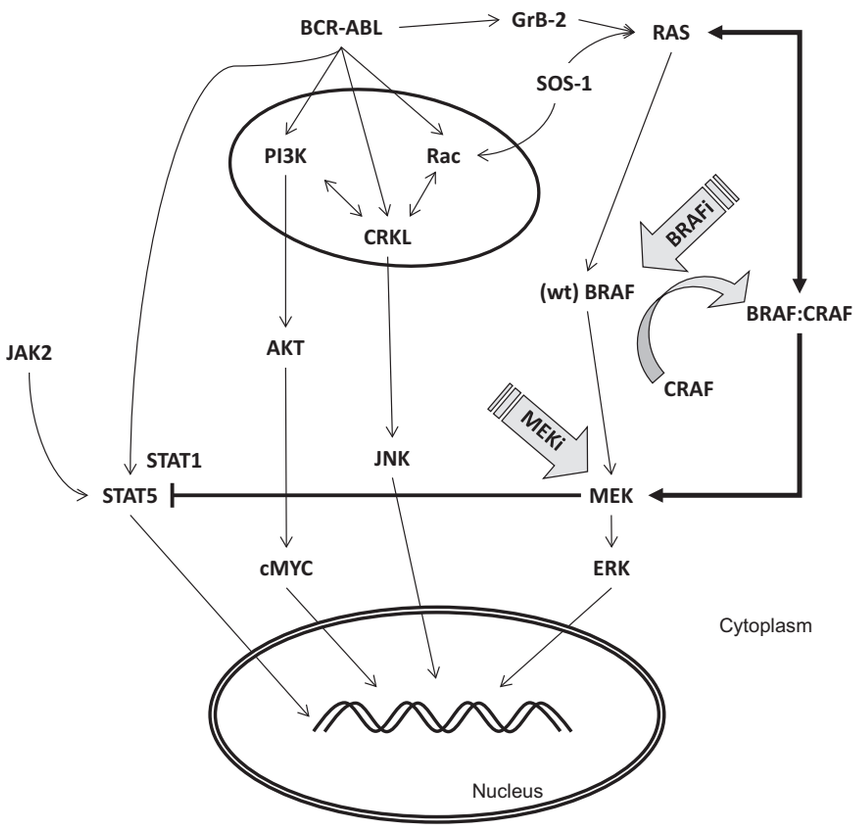

Figure 6.
Selected interacting molecules and signal transduction pathways acting downstream of BCR–ABL1. Paradoxical activation of wild-type (wt) BRAF in the presence of activated RAS and a BRAF inhibitor (BRAFi) such as dabrafenib leads to BRAF-CRAF heterodimerization (curved arrow), translocation to the cell-surface and activation by RAS (dashed double-headed arrow) with consequent CRAF-mediated activation of MEK. MEK inhibition (MEKi) by drugs, such as trametinib, prevents MEK-directed activation of ERK and relieves MEK-dependent negative feedback on STAT5 (blunt-ended arrow).

Another study reported a novel CRAF dysregulation mechanism that would, theoretically, be amenable to MEK/ERK inhibition (26). The proapoptotic molecule BIM is known to be an important mediator of the response to imatinib in CML; we did not find a consistent change in BIM expression in three model CML cell lines in response to dabrafenib/trametinib, suggesting that while differences exist between the cell lines, BIM is unlikely to represent a critical role in the beneficial hematologic effects of MAPK targeting in this setting (27, 28).

These findings are interesting considering what is known about the paradoxical MAPK-activating effects of BRAF inhibitors in cells that are wild-type for *BRAF*. As we and others have previously reported, MAPK-activated cells, commonly those harboring oncogenic *RAS* mutations, may in fact be stimulated to proliferate when exposed to V600 mutation-selective BRAF inhibitors (7, 29). Insofar as RAS appears to be a downstream target of BCR–ABL1, CML cells may thus be considered RAS-activated and therefore susceptible to BRAF inhibitor-driven proliferation (Fig. 6). Furthermore, CML cells with acquired resistance to BCR–ABL1–targeted kinase inhibitors may also display paradoxical MAPK activation. This has been observed in CML cells harboring the common BCR-ABL^{T315I} secondary-resistance mutation during continued exposure to kinase inhibitors such as imatinib, due to weak off-target binding of inhibitor to BRAF. This phenomenon could be exploited by the addition of a MEK inhibitor, which appeared to induce synthetic lethality in this context (6).

Interacting partners and downstream modulators of BCR–ABL1 signaling are numerous and include RAC and RHO family members, STAT5, CRKL, and the PI3K/AKT pathway in addition to MAPK members. BCR–ABL1 activates MAPK signaling in a GRB2 and SOS-1–dependent manner (24, 30–36), but leads to marked MEK-dependent negative feedback of receptor-level growth factor signaling, as well as direct negative feedback on RAS itself (Fig. 6; ref. 25). Although we did not find a significant direct effect of dabrafenib or trametinib on BCR–ABL1 activation as measured by phosphorylation of ABL-Tyr245 and CRKL, possibly due to the kinetics of our assay, we found clear evidence that dabrafenib dose-dependently reduced STAT5 phosphorylation. This effect was likely due to paradoxical activation of MEK in the context of BRAF inhibitor monotherapy, with consequent intensification of MEK-dependent negative feedback on STAT5 phosphorylation, as has been described in other studies (25). Although trametinib cotreatment had a very small counter-effect on STAT5 phosphorylation, trametinib monotherapy had little effect on STAT5 phosphorylation relative to untreated cells (Supplementary Fig. S2). This suggests that the set-point of this feedback loop is such that negligible negative feedback on STAT5 occurs until MEK activity is raised above basal levels, in this case by dabrafenib. Whether some of the functional differences observed between BRAF monotherapy and combined BRAF/MEK inhibition may relate to this divergent effect on STAT5, either in preference or in addition to divergent effects on MAPK pathway signaling, is unclear and warrants further investigation.

In our case, despite complete hematologic response, there was no significant decline in *BCR–ABL1* gene expression either in blood or by repeat bone marrow cytogenetics, indicating that MEK inhibition was not effective at inducing molecular or cytogenetic response. Given the clear relationship between depth of molecular response and long-term outcome in CML (16), MEK inhibition as a single-agent therapy would thus seem unsuitable, but could be considered in combination with other therapies, or potentially in cases of therapeutic resistance such as the BCR–ABL1 T315I mutation, for which current first- and second-generation BCR–ABL1 kinase inhibitors are ineffective (37–39). Although unintended MAPK activation may be undesirable in other cancer settings, it may paradoxically be advantageous in therapy-resistant CML by driving cells into the downstream proapoptotic block afforded by concurrent MEK inhibition. Exactly how dependent the efficacy of this approach is on the degree of upstream MAPK activation is unclear and may influence its therapeutic potential.

Conclusion

This case documents a unique observation of complete hematologic response to MEK inhibition in a patient with chronic-phase CML and concomitant metastatic melanoma. It confirms differential effects of MEK inhibition on defined leukocyte subsets, highlighting the inhibitory effects on CML cell proliferation and colony formation. Although previous preclinical work suggests a role for MEK inhibition in acquired BCR–ABL1 inhibitor resistance, the response seen in our patient occurred without prior exposure to, or selection against, imatinib or related kinase inhibitors. These findings may support a more prominent therapeutic role for MAPK targeting in CML that is not limited to exploitation of paradoxical MAPK activation seen in some drug-resistant CML populations. MEK inhibition appears to affect a broad spectrum of hematopoietic lineages in CML, but our correlative analyses indicate that its primary clinically relevant effect may be on a primitive subpopulation. Further clinical evaluation of MAPK targeting as add-on therapy to conventional BCR–ABL1 kinase inhibitors, and in the setting of resistance to these agents is warranted.

Disclosure of Potential Conflicts of Interest

M.C. Andrews is a consultant/advisory board member for GlaxoSmithKline. No potential conflicts of interest were disclosed by the other authors.

Authors' Contributions

Conception and design: M.C. Andrews, N. Turner, A.W. Roberts, A. Behren, J. Cebon

Development of methodology: M.C. Andrews, A. Behren

Acquisition of data (provided animals, acquired and managed patients, provided facilities, etc.): M.C. Andrews, N. Turner, J. Boyd, A.W. Roberts, A.P. Grigg, J. Cebon

Analysis and interpretation of data (e.g., statistical analysis, biostatistics, computational analysis): M.C. Andrews, N. Turner, J. Boyd, A.W. Roberts, A. Behren

Writing, review, and/or revision of the manuscript: M.C. Andrews, N. Turner, J. Boyd, A.W. Roberts, A.P. Grigg, A. Behren

Administrative, technical, or material support (i.e., reporting or organizing data, constructing databases): J. Boyd

Study supervision: A. Behren, J. Cebon

Other (involved in decisions care of the patients and extensively reviewed and revised the manuscript on more than one occasion): A.P. Grigg

Acknowledgments

The authors thank the patient and his family for their support of this work; Tina Cavicchiolo and Noel Micallef for expert clinical trial management; Nektaria Dimopoulos and James Lynam for their assistance and insights with flow cytometry; Laura J. Vella for guidance with Western blotting, and Hongdo Do for HRM analysis.

Grant Support

M.C. Andrews is supported by a National Health and Medical Research Council of Australia Postgraduate Medical Scholarship (#1055456) and A.W. Roberts by a Practitioner Fellowship (#637309) and Program Grant (#1016647). This work was funded in part by Ludwig Cancer Research, and Operational Infrastructure Support Program funding of the Victorian State Government.

The costs of publication of this article were defrayed in part by the payment of page charges. This article must therefore be hereby marked *advertisement* in accordance with 18 U.S.C. Section 1734 solely to indicate this fact.

Received February 17, 2015; revised July 14, 2015; accepted July 14, 2015; published OnlineFirst July 22, 2015.

References

1. Rowley JD. Letter: a new consistent chromosomal abnormality in chronic myelogenous leukaemia identified by quinacrine fluorescence and Giemsa staining. Nature 1973;243:290–3.
2. Shtivelman E, Lifshitz B, Gale RP, Canaani E. Fused transcript of abl and bcr genes in chronic myelogenous leukaemia. Nature 1985;315: 550–4.
3. Druker BJ. Molecularly targeted therapy: have the floodgates opened? Oncologist 2004;9:357–60.
4. Lyubynska N, Gorman MF, Lauchle JO, Hong WX, Akutagawa JK, Shannon K, et al. A MEK inhibitor abrogates myeloproliferative disease in Kras mutant mice. Sci Transl Med 2011;3:76ra27.
5. Chang T, Krisman K, Theobald EH, Xu J, Akutagawa J, Lauchle JO, et al. Sustained MEK inhibition abrogates myeloproliferative disease in Nf1 mutant mice. J Clin Invest 2013;123:335–9.
6. Packer LM, Rana S, Hayward R, O'Hare T, Eide CA, Rebocho A, et al. Nilotinib and MEK inhibitors induce synthetic lethality through paradoxical activation of RAF in drug-resistant chronic myeloid leukemia. Cancer Cell 2011;20:715–27.
7. Callahan MK, Rampal R, Harding JJ, Klimek VM, Chung YR, Merghoub T, et al. Progression of RAS-mutant leukemia during RAF inhibitor treatment. N Engl J Med 2012;367:2316–21.
8. Flaherty KT, Infante JR, Daud A, Gonzalez R, Kefford RF, Sosman J, et al. Combined BRAF and MEK inhibition in melanoma with BRAF V600 mutations. N Engl J Med 2012;367:1694–703.
9. Grigg AP, Roberts AW, Raunow H, Houghton S, Layton JE, Boyd AW, et al. Optimizing dose and scheduling of filgrastim (granulocyte colony-stimulating factor) for mobilization and collection of peripheral blood progenitor cells in normal volunteers. Blood 1995;86:4437–45.
10. Balch CM, Gershenwald JE, Soong SJ, Thompson JF, Atkins MB, Byrd DR, et al. Final version of 2009 AJCC melanoma staging and classification. J Clin Oncol 2009;27:6199–206.
11. Oken MM, Creech RH, Tormey DC, Horton J, Davis TE, McFadden ET, et al. Toxicity and response criteria of the Eastern Cooperative Oncology Group. Am J Clin Oncol 1982;5:649–55.
12. Schniewind B, Christgen M, Hauschild A, Kurdow R, Kalthoff H, Klomp HJ. Paraneoplastic leukemoid reaction and rapid progression in a patient with malignant melanoma: establishment of KT293, a novel G-CSF-secreting melanoma cell line. Cancer Biol Ther 2005;4: 23–7.
13. Eisenhauer EA, Therasse P, Bogaerts J, Schwartz LH, Sargent D, Ford R, et al. New response evaluation criteria in solid tumours: revised RECIST guideline (version 1.1). Eur J Cancer 2009;45:228–47.
14. Druker BJ, Guilhot F, O'Brien SG, Gathmann I, Kantarjian H, Gattermann N, et al. Five-year follow-up of patients receiving imatinib for chronic myeloid leukemia. N Engl J Med 2006;355:2408–17.
15. O'Brien SG, Guilhot F, Larson RA, Gathmann I, Baccarani M, Cervantes F, et al. Imatinib compared with interferon and low-dose cytarabine for newly diagnosed chronic-phase chronic myeloid leukemia. N Engl J Med 2003;348:994–1004.
16. Hochhaus A, O'Brien SG, Guilhot F, Druker BJ, Branford S, Foroni L, et al. Six-year follow-up of patients receiving imatinib for the first-line treatment of chronic myeloid leukemia. Leukemia 2009;23: 1054–61.
17. O'Brien SG, Guilhot F, Goldman JM, Hochhaus A, Hughes TP, Radich JP, et al. International randomized study of interferon versus STI571 (IRIS) 7-year follow-up: sustained survival, low rate of transformation and increased rate of major molecular response (MMR) in patients (pts) with newly diagnosed chronic myeloid leukemia in chronic phase (CMLCP) treated with imatinib (IM). Blood (ASH Annual Meeting Abstracts). 2008 112: Abstract 186.
18. Mathisen MS, Kantarjian HM, Cortes J, Jabbour EJ. Practical issues surrounding the explosion of tyrosine kinase inhibitors for the management of chronic myeloid leukemia. Blood Rev 2014;28: 179–87.
19. Nguyen TK, Rahmani M, Gao N, Kramer L, Corbin AS, Druker BJ, et al. Synergistic interactions between DMAG and mitogen-activated protein kinase kinase 1/2 inhibitors in Bcr/abl+ leukemia cells sensitive and resistant to imatinib mesylate. Clin Cancer Res 2006; 12:2239–47.
20. Nguyen TK, Rahmani M, Harada H, Dent P, Grant S. MEK1/2 inhibitors sensitize Bcr/Abl+ human leukemia cells to the dual Abl/Src inhibitor BMS-354/825. Blood 2007;109:4006–15.
21. Yu C, Dasmahapatra G, Dent P, Grant S. Synergistic interactions between MEK1/2 and histone deacetylase inhibitors in BCR/ABL$^+$ human leukemia cells. Leukemia 2005;19:1579–89.
22. Yu C, Krystal G, Varticovksi L, McKinstry R, Rahmani M, Dent P, et al. Pharmacologic mitogen-activated protein/extracellular signal-regulated kinase kinase/mitogen-activated protein kinase inhibitors interact synergistically with STI571 to induce apoptosis in Bcr/Abl-expressing human leukemia cells. Cancer Res 2002;62:188–99.
23. Kang CD, Do IR, Kim KW, Ahn BK, Kim SH, Chung BS, et al. Role of Ras/ERK-dependent pathway in the erythroid differentiation of K562 cells. Exp Mol Med 1999;31:76–82.
24. Redig AJ, Vakana E, Platanias LC. Regulation of mammalian target of rapamycin and mitogen activated protein kinase pathways by BCR-ABL. Leuk Lymphoma 2011;52(Suppl 1):45–53.
25. Asmussen J, Lasater EA, Tajon C, Oses-Prieto J, Jun YW, Taylor BS, et al. MEK-dependent negative feedback underlies BCR-ABL–mediated oncogene addiction. Cancer Discov 2014;4:200–15.
26. Hentschel J, Rubio I, Eberhart M, Hipler C, Schiefner J, Schubert K, et al. BCR-ABL$^-$ and Ras-independent activation of Raf as a novel mechanism of Imatinib resistance in CML. Int J Oncol 2011;39: 585–91.
27. Kuroda J, Puthalakath H, Cragg MS, Kelly PN, Bouillet P, Huang DC, et al. Bim and Bad mediate imatinib-induced killing of Bcr/Abl+ leukemic cells, and resistance due to their loss is overcome by a BH3 mimetic. Proc Natl Acad Sci U S A 2006;103:14907–12.
28. Ng KP, Hillmer AM, Chuah CT, Juan WC, Ko TK, Teo AS, et al. A common BIM deletion polymorphism mediates intrinsic resistance and inferior responses to tyrosine kinase inhibitors in cancer. Nat Med 2012;18: 521–8.
29. Andrews MC, Behren A, Chionh F, Mariadason J, Vella LJ, Do H, et al. BRAF inhibitor-driven tumor proliferation in a KRAS-mutated colon carcinoma is not overcome by MEK1/2 inhibition. J Clin Oncol 2013;31:e448–51.
30. Mizuchi D, Kurosu T, Kida A, Jin ZH, Jin A, Arai A, et al. BCR/ABL activates Rap1 and B-Raf to stimulate the MEK/Erk signaling pathway in hematopoietic cells. Biochem Biophys Res Commun 2005; 326:645–51.
31. Nakamura S. Bcr-abl-mediated Raf kinase inhibitor protein suppression promotes chronic myeloid leukemia progenitor cells proliferation. Stem Cell Discov 2011;1:54–66.
32. Platanias LC. MAP kinase signaling pathways and hematologic malignancies. Blood 2003;101:4667–79.
33. Quintas-Cardama A, Cortes J. Molecular biology of bcr-abl1-positive chronic myeloid leukemia. Blood 2009;113:1619–30.
34. Steelman LS, Pohnert SC, Shelton JG, Franklin RA, Bertrand FE, McCubrey JA. JAK/STAT, Raf/MEK/ERK, PI3K/Akt and BCR-ABL in cell cycle progression and leukemogenesis. Leukemia 2004;18:189–218.
35. Modi H, Li L, Chu S, Rossi J, Yee JK, Bhatia R. Inhibition of Grb2 expression demonstrates an important role in BCR-ABL-mediated MAPK activation

and transformation of primary human hematopoietic cells. Leukemia 2011;25:305–12.
36. Puil L, Liu J, Gish G, Mbamalu G, Bowtell D, Pelicci PG, et al. Bcr-Abl oncoproteins bind directly to activators of the Ras signalling pathway. EMBO J 1994;13:764–73.
37. Jabbour E, Cortes JE, Giles FJ, O'Brien S, Kantarjian HM. Current and emerging treatment options in chronic myeloid leukemia. Cancer 2007;109:2171–81.
38. O'Hare T, Eide CA, Deininger MW. Bcr-Abl kinase domain mutations, drug resistance, and the road to a cure for chronic myeloid leukemia. Blood 2007;110:2242–9.
39. von Bubnoff N, Manley PW, Mestan J, Sanger J, Peschel C, Duyster J. Bcr-Abl resistance screening predicts a limited spectrum of point mutations to be associated with clinical resistance to the Abl kinase inhibitor nilotinib (AMN107). Blood 2006;108: 1328–33.

Published OnlineFirst July 22, 2015; DOI: 10.1158/1078-0432.CCR-15-0393

Clinical Cancer Research

Cellular Mechanisms Underlying Complete Hematological Response of Chronic Myeloid Leukemia to BRAF and MEK1/2 Inhibition in a Patient with Concomitant Metastatic Melanoma

Miles C. Andrews, Natalie Turner, Janis Boyd, et al.

Clin Cancer Res 2015;21:5222-5234. Published OnlineFirst July 22, 2015.